Int. J. Heat Mass Transfer. Vol. 30, No. 5, pp. 911–926, 1987
Printed in Great Britain

0017–9310/87 $3.00 + 0.00
Pergamon Journals Ltd.

# Reynolds analogies and experimental study of heat transfer in the supersonic boundary layer

J. GAVIGLIO

Institut de Mécanique Statistique de la Turbulence (I.M.S.T.), 12, Avenue Général Leclerc, 13003 Marseille, France

(*Received* 10 *March* 1986)

**Abstract**—Supersonic flows cannot be calculated using the classical Reynolds analogy, which must be replaced with a more specific one. The 'strong Reynolds analogy', due to Young and Morkovin, fulfills this role approximately if the wall is quasi-adiabatic, but not if a significant heat flux is present. To overcome this situation, another more general representation is proposed. Based on results involving the role of large-scale movements present in the boundary layer, this schematic model draws a relationship between temperature and velocity turbulent intensities and mean flow characteristics, while also examining the role of compressibility in turbulent motion.

## 1. INTRODUCTION

### 1.1. *Review of subject*

IN RECENT years, the study of the relationship between velocity and temperature has taken on great importance due to the influence of intense heating at the wall on the development of boundary layers. Such is the case, for example, for aircraft flying at supersonic speeds, where increasingly powerful jet engines provide heat sources capable of affecting the dynamic properties of boundary layers. The heat source modifies the curvature of streamlines as well as the pressure distribution, thereby generating zones of compression and relaxation, which can affect flight stability. As suggested by Cebeci and Bradshaw (ref. [1], p. 41), these flows will be referred to as 'coupled flows', characterized as compressible with variable density, while the term 'uncoupled flows' will be used to denote incompressible flows occurring at low speeds where density is almost constant and heat is only a passive contaminant.

To calculate uncoupled flows, specialists in aerodynamics use the well-known Reynolds analogy, hereafter referred to as the analogy of the first kind (or 'première manière', cf. Gaviglio, in Favre *et al.* [2], Chap. V, par. 2.3) which stipulates that turbulence-induced transfers of momentum and heat occurring normal to the wall take place in the same manner (Brun *et al.* [3], Vol. 3, p. 197). This analogy relates heat convection results to friction, which is often easier to measure. Boundary layers in supersonic flow, however, are 'coupled flows', even in the absence of a heat source or sink at the wall. Turbulence dissipates energy through viscous friction within the flow itself, thereby explaining the existence of mean enthalpy gradients. The analogy of the first kind can therefore no longer be applied in such a straightforward manner. Furthermore, directly measured temperature is equal to the local isentropic total temperature, complicating both experiments and equations. Calculations therefore call upon approximate solutions, due to Young [4], consisting of complex equations, and reformulated relations discussed and applied by Morkovin [5] who designated them as the 'strong Reynolds analogy' (SRA), hereafter referred to as the analogy of the second kind (or 'deuxième manière', cf. ref. [2]).

This paper examines the above analogies and highlights the difficulties encountered in their concept and use. It also suggests a way to avoid these problems by establishing a new schematic model that allows the effects of compressibility, and its probable causes, to be examined.

### 1.2. *Basic hypotheses and conditions of the study*

(a) The study has been limited to continuous, two-dimensional equilibrium boundary layer turbulent flows, at a moderate external Mach number of $M_e \lesssim 5$. Equations are written in the mass-weighted average form (cf. Favre *et al.* [2], Chap. II) since this type of notation contains fewer terms than the Reynolds representation, and the physical meaning is clearer. Each instantaneous quantity $W$ is separated into its mean value $\tilde{W}$ and its fluctuation such that $W = \tilde{W} + W'$, $\tilde{W} = \overline{\rho w}/\bar{\rho}$ and $W'' = -\overline{\rho' w''}/\bar{\rho}$. Mean equations of continuity and state are

$$\frac{\partial \bar{\rho}\tilde{u}}{\partial x} + \frac{\partial \bar{\rho}\tilde{v}}{\partial y} = 0 \tag{1}$$

$$\bar{p} = R\bar{\rho}\tilde{T}. \tag{2}$$

For a moderate Mach number, and at any point P in the boundary layer (Fig. 1), it is assumed in a first approximation (Sections 1–3), that fluctuations of velocity $\mathbf{q}'$ are primarily rotational ($u' \simeq u'_\omega$) while fluctuations of temperature $T'$ are primarily isobaric. This implies that pressure fluctuations are neglected. The fluctuating temperature field is therefore practi-

## NOMENCLATURE

| | |
|---|---|
| $a$ | speed of sound |
| $c_p$, $c_v$ | specific heat of air at constant pressure and constant volume, respectively |
| D | derivative symbol, $D/Dt = \partial/\partial t + u_i(\partial/\partial x_j)$ |
| $h$ | static enthalpy, $c_pT$ |
| $H$ | total enthalpy, $c_pT_t$ |
| $i, j, k$ | directions in a reference frame |
| $k$ | wave number, $2\pi n/\tilde{u}$ |
| $l, L$ | length scales |
| $M$ | Mach number |
| $n$ | frequency |
| $p$ | pressure |
| $Pr$ | molecular Prandtl number |
| $Pr_t$ | turbulent Prandtl number |
| $\mathbf{q}$ | instantaneous velocity (modulus $\tilde{q}$): $\mathbf{u} + \mathbf{v} + \mathbf{w}$ |
| $Q$ | heat flux: at the wall, $Q_w = \lambda(\partial\tilde{T}/\partial y)_w = \lambda(\partial\tilde{T}_t/\partial y)_w$ |
| $R$ | constant characteristic of perfect gases, $c_p - c_v$ |
| $R_{uT}$, $R_{Tv}$, $R_{uv}$ | correlation coefficient between $u'$ and $T'$, between $T'$ and $v'$, and between $u'$ and $v'$ |
| $\mathscr{R}$ | Reynolds number |
| $t$ | time |
| $T$ | gas temperature (of a particle) |
| $T_e$ | gas temperature (of a particle) in the outer flow |
| $T_t$ | isentropic total temperature |
| $T_f$ | 'friction' temperature: $T_e(1 + Pr^{1/3}((\gamma - 1)/2)M_e^2)$ |
| $T'_n$ | fluctuation temperature $T'$ filtered in a narrow frequency band |
| $T_w$ | wall temperature |
| $u, v, w$ | instantaneous components of velocity in the $x$-, $y$- and $z$-directions respectively (cf. Fig. 1) |
| $u'_n$ | fluctuation velocity $u'$ filtered in a narrow frequency band |
| $W$ | instantaneous quantity separated into its average and its fluctuation, $\tilde{W} + W'$ |
| $x, y, z$ | distances, cf. Fig. 1. |

Greek symbols

| | |
|---|---|
| $\gamma$ | $(c_p/c_v)$ |
| $\delta$ | conventional boundary layer thickness |
| $\bar{\delta}$ | r.m.s. thickness |
| $\delta^*$ | displacement thickness |
| $\Delta$ | finite difference |
| $\theta$ | momentum thickness |
| $\lambda$ | coefficient of heat conductivity of the gas |
| $\mu$ | coefficient of static viscosity of the gas |
| $\rho$ | gas density |
| $\rho u$ | momentum |
| $\tau$ | friction: at the wall, $\tau_w = \mu(\partial\tilde{u}/\partial y)_w$ |
| $\Phi$ | mean energy dissipation through viscous friction. |

Subscripts

| | |
|---|---|
| d | dissipation |
| e | external (outside the boundary layer) |
| ir | irrotational |
| is | isentropic |
| n | narrow band filtering, e.g. $u'_n$, $T'_n$, $(R_{uT})_n$ |
| r | in a relative movement |
| s | non-isentropic |
| t | turbulent, e.g. $(Pr_t)$; or relative to total temperature, e.g. $(T_t)$ |
| w | relative to the wall $(y = 0)$ |
| $\omega$ | rotational. |

Superscripts

| | |
|---|---|
| $\bar{(\ )}$ | statistical average |
| $\tilde{(\ )}$ | mass-weighted average |
| $\hat{(\ )}$ | dimensionless quantity |
| $(\ )'$ | fluctuation. |

cally non-isentropic ($T' \simeq T'_s$). The fluctuations $u'$ and $T'$ are assumed to be convected by the mean flow velocity according to the simplified theory of 'modes of turbulence' [6] which categorizes fluctuations as 'rotational', 'entropic', and 'sound'. Results from a large number of experiments substantiate this point of view [5, 7, 8]. In this case, linearized equations of continuity and state for fluctuations are written as

$$\frac{\partial u'}{\partial x} + \frac{\partial v'}{\partial y} + \frac{\partial w'}{\partial z} = 0 \tag{3}$$

$$\frac{p'}{\bar{p}} = \frac{\rho'}{\bar{\rho}} + \frac{T'}{\bar{T}} \tag{4}$$

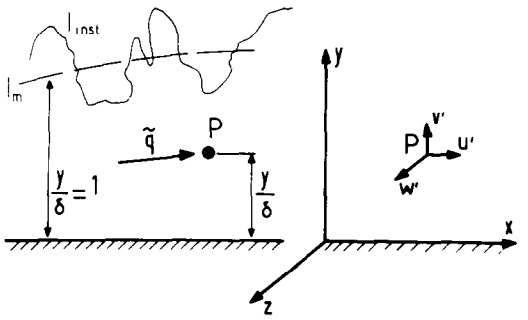


FIG. 1. Boundary layer. Sketch of the flow. Frame of reference. $l_{inst}$, instantaneous superlayers; $l_m$, conventional mean boundary layer.

where

$$\frac{p'}{\bar{p}} \ll \frac{\rho'}{\bar{\rho}}, \frac{T'}{\tilde{T}} \tag{5}$$

or

$$\frac{\rho'}{\bar{\rho}} \simeq -\frac{T'}{\tilde{T}}. \tag{6}$$

These approximations become less reliable as the external Mach number $M_e$ increases. In a second approximation (Section 4) pressure fluctuations will be shown to play an explicit role.

(b) It is assumed that for any value of $y/\delta$, the modulus $\tilde{q}$ of the mean velocity vector differs only slightly from the $\tilde{u}$ component parallel to the wall, and from the particulate velocity $\bar{u}$. The velocity component, $\tilde{u}$, or $\bar{u}$, is measured by means of pressure tubes or by laser Doppler velocimetry (LDV). The latter also provides the component $\bar{v}$ ($\simeq \tilde{v}$, deducible from equation (1) if the flow is truly two-dimensional) as well as fluctuations $u'$ and $v'$. The fluctuation $u'$ is also obtained using a 'straight' hot-wire probe, i.e. normal to the mean flow. A yawed wire probe inclined on the mean flow, or a probe formed by two crossed wires is used to measure $v'$, although accuracy of the latter is often mediocre. Lastly, a 'straight' hot-wire anemometer is used to characterize the total temperature field $T_t = \tilde{T}_t + T_t'$ and the temperature field $T = \tilde{T} + T'$ using the well-known fluctuation diagram method [6] that also provides standard deviations $\sqrt{(\overline{u'^2})}$ and $\sqrt{(\overline{T'^2})}$ as well as the correlation coefficient $R_{uT}$. As for the thermal field, given the temperature range of $100\,\mathrm{K} < \tilde{T} < 1000\,\mathrm{K}$, it is assumed that specific heat values $c_p$ and $c_v$, the dynamic viscosity coefficient, and thermal conductivity of the air remain practically constant.

(c) Section 2 recalls the basic ideas of the first Reynolds analogy, and then those of the SRA. Certain difficulties in interpretation are pointed out, together with inherent limitations from an application viewpoint, namely in cases where there exists an intense heat flux at the wall. To overcome these shortcomings, Section 3 proposes another form of analogy that takes into account the effects of compressibility on the mean flow field. Effects of compressibility on the turbulent field are examined in Section 4.

## 2. REYNOLDS ANALOGIES

### 2.1. *The Reynolds analogy of the first kind*

For any external Mach number $M_e$, the mean momentum and mean enthalpy equations are

$$\bar{\rho}\left(\tilde{u}\frac{\partial\tilde{u}}{\partial x} + \tilde{v}\frac{\partial\tilde{u}}{\partial y}\right) = -\frac{\partial\bar{p}}{\partial x} + \frac{\partial}{\partial y}\left(\mu\frac{\partial\tilde{u}}{\partial y} - \bar{\rho}\overline{u'v'}\right) \tag{7a}$$

$$c_p\bar{\rho}\left(\tilde{u}\frac{\partial\tilde{T}}{\partial x} + \tilde{v}\frac{\partial\tilde{T}}{\partial y}\right) = \tilde{u}\frac{\partial\bar{p}}{\partial x} - \frac{\overline{\rho'u'}}{\bar{\rho}}\frac{\partial\bar{p}}{\partial x} + \overline{u_i'\frac{\partial p'}{\partial x_i}} + \frac{\partial}{\partial y}\left(\lambda\frac{\partial\tilde{T}}{\partial y} - c_p\bar{\rho}\overline{v'T'}\right) + \Phi. \tag{8a}$$

For equilibrium incompressible flows, $\partial\bar{p}/\partial x = 0$, wherein density varies as a function of distance from the wall, turbulent exchanges of momentum and heat predominate over molecular exchanges outside the viscous sublayer. Since dissipation is negligible, the above equations may be simplified in the conventional manner (cf. ref. [1], pp. 46–50) to

$$\bar{\rho}\left(\tilde{u}\frac{\partial\tilde{u}}{\partial x} + \tilde{v}\frac{\partial\tilde{u}}{\partial y}\right) = -\frac{\partial}{\partial y}\bar{\rho}\overline{u'v'} \tag{7b}$$

$$c_p\bar{\rho}\left(\tilde{u}\frac{\partial\tilde{T}}{\partial x} + \tilde{v}\frac{\partial\tilde{T}}{\partial y}\right) = -c_p\frac{\partial}{\partial y}\bar{\rho}\overline{v'T'}. \tag{8b}$$

If boundary conditions are analogous (i.e. if mean velocity and mean temperature have similar distributions) and if the Prandtl number $Pr = \mu c_p/\lambda$ remains close enough to 1, these equations give the solutions

$$\frac{T_w - \tilde{T}}{T_w - T_e} = \frac{\tilde{u}}{u_e} \tag{9}$$

$$\frac{-T'}{T_w - T_e} = \frac{u'}{u_e}. \tag{10}$$

Equations (9) and (10) characterize an 'exact analogy', as pointed out by Cebeci and Bradshaw [1]. This analogy would therefore apply to an ideal, i.e. unrealistic, situation. The attenuated form

$$\frac{\sqrt{(\overline{T'^2})}}{T_w - T_e} \simeq \frac{\sqrt{(\overline{u'^2})}}{u_e} \tag{11}$$

derived from equations (9) and (10) appears less questionable, as it does not formulate such a strict relation between $u'$ and $T'$ as do the other equations.

This relation could only exist if the scattering induced by the $v'$ and $w'$ components were neglected, along with the effects of pressure fluctuations.

### 2.2. *The analogy of the second kind or strong Reynolds analogy (SRA)*

2.2.1. *Equations.*

(a) For supersonic flows equation (7a) holds, but since dissipation plays a major role, equation (8a) cannot be simplified. In order to obtain new formal solutions, it is possible to use the equation representing the evolution of mean total enthalpy. Instantaneous total enthalpy is defined by

$$H = c_p T_t = h + \frac{q^2}{2} = c_p T + \frac{q^2}{2}. \tag{12}$$

This equation can be rearranged and simplified as follows (cf. ref. [1], p. 49):

$$\tilde{H} + H' = c_p \tilde{T}_t + c_p T_t' = \left(c_p \tilde{T} + \frac{\tilde{u}^2}{2}\right) + \left(T' + \frac{\tilde{u}}{c_p} u'\right) \tag{13}$$

$$\tilde{H} = c_p \tilde{T}_t \simeq c_p \tilde{T} + \frac{\tilde{u}^2}{2} \tag{14}$$

$$H' \simeq c_p T' + \tilde{u} u' = c_p T_t'. \tag{15}$$

The equation that governs this relation is obtained by adding the equations for mean enthalpy $\tilde{h} = c_p \tilde{T}$, mean kinetic energy, and turbulent kinetic energy, which gives

$$c_p \bar{\rho}\left(\tilde{u}\frac{\partial \tilde{T}_t}{\partial x} + \bar{v}\frac{\partial \tilde{T}_t}{\partial y}\right) = \frac{\partial}{\partial y}\left\{\lambda\left[\frac{\partial \tilde{T}_t}{\partial y} + \frac{Pr - 1}{c_p}\frac{\partial}{\partial y}\left(\frac{\tilde{u}^2}{2}\right)\right] - c_p \bar{\rho}\overline{v' T_t'}\right\}. \tag{16}$$

This equation no longer contains the dissipation term, nor any pressure term. Young [4] has established a comparison between equations (7a) and (16) in which he assumes that molecular effects are negligible, while at the same time $Pr = 1$. He considers several different situations.

First case: the wall is heated or cooled and no pressure gradients are present. $Q_w \neq 0$; $\partial \bar{p}/\partial x = 0$.

In this case the equations have the same form and boundary conditions are analogous: at the wall $\tilde{T}_t - \tilde{T}_{tw} = 0$, $\tilde{u} = 0$; at the free boundary $T_t - T_w = T_{te} - T_w$, $\tilde{u} = u_e$. For these formal reasons, the author admits the double solution

$$c_p \tilde{T}_t - T_w = k_1 \tilde{u} \tag{17a}$$

$$c_p T_t' = k_1 u' \tag{17b}$$

where $k_1$ is a constant deduced from conditions at the wall

$$Q_w = -\lambda\left(\frac{\partial \tilde{T}_t}{\partial y}\right)_w, \qquad \tau_w = \mu\left(\frac{\partial \tilde{u}}{\partial y}\right)_w.$$

Morkovin [5] specifies $k_1$ in the form $k_1 = Pr_w(Q_w/\tau_w)$.

Second case: the wall is adiabatic and no pressure gradients are present. $Q_w = 0$; $\partial \bar{p}/\partial x = 0$.

In this case $k_1$ is nil and the double solution is

$$T_t = 0 \Leftrightarrow \begin{cases} \tilde{T}_t = T_w = c^{te} & \text{(18a)} \\ T_t' = 0 = T' + \dfrac{\tilde{u}}{c_p} u'. & \text{(18b)} \end{cases}$$

Morkovin writes relations (18a) and (18b) in the form

$$\sqrt{(\overline{T_t'^2})} = 0 \tag{19}$$

$$\sqrt{(\overline{T'^2})} = \frac{\tilde{u}}{c_p}\sqrt{(\overline{u'^2})} \tag{20}$$

equal to

$$\frac{\sqrt{(\overline{T'^2})}/\tilde{T}}{(\gamma - 1)M^2(\sqrt{(\overline{u'^2})}/\tilde{u})} \simeq 1 \tag{21}$$

$$-R_{uT} = 1. \tag{22}$$

Third case: the wall is adiabatic and the pressure gradient is different than zero. $Q_w = 0$; $\partial \bar{p}/\partial x \neq 0$.

Solutions (18a) and (18b) satisfy equation (16) considered independently; they may therefore be applied for any value of $\partial \bar{p}/\partial x$. Solutions (17)–(22) are referred to as 'SRA relations'.

(b) As for solutions (9) and (10), and for the same reasons, these relations describe an 'exact' analogy, i.e. one that may be applied to an ideal boundary case, which most likely explains why this analogy has been qualified as 'strong'.

(c) In the case of a weak heat flux at the wall, solution (17b) may serve as a basis for establishing solutions such as (18)–(22). Cebeci and Smith (ref. [9], p. 71) obtain one of these solutions by postulating that the Crocco relation between $\tilde{u}$, $\tilde{T}$ and $\tilde{T}_t$ is valid. These authors' results give

$$\frac{\sqrt{(\overline{T'^2})}/\tilde{T}}{(\gamma - 1)M^2\sqrt{(\overline{u'^2})}/\tilde{u}} \simeq 1 + c_p \frac{T_w - T_{te}}{\tilde{T}}\frac{\tilde{u}}{u_e}. \tag{23}$$

It is possible to verify that the theoretical and numerical results are close to those given in equation (23) by using semi-empirical equations relating $Q_w$ to $\tau_w$, such as those provided in ref. [10], Vol. 2, pp. 128–130. This is true because the equations given above, as well as the Crocco relation, are all valid in equilibrium flows. Equation (23) will hereafter be referred to as the 'extended SRA solution'.

2.2.2. *Experimental testing of the SRA relations.* Figure 2 shows an example (partly shown in Dussauge

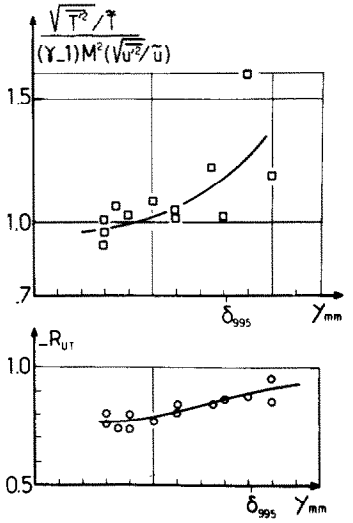


FIG. 2. Test of the strong Reynolds analogy relations.

[11]) from experimental testing of relations of the analogy of the second kind for an equilibrium boundary layer at supersonic speeds on a non-heated† (quasi-adiabatic) wall. Equation (21) is valid for the non-intermittent zone $0.05 < y/\delta < 0.7$, but the same is not true for equation (22) since $(-R_{uT})$ differs from 1 by about 15–25%. In ref. [7], slightly greater deviations were found for other Mach numbers. These observations merit several remarks.

(a) The reasons for the above-mentioned differences are the same as those indicated in par. 2.1. In addition, Young (1986, private communication) points out that the term in $(Pr-1)$, neglected in equation (16), represents a measurement of the dissimilarity of the two different modes of transfer for vector $\rho\mathbf{u}$ and scalar $T_t$ which do not respond in the same manner to changes in density and pressure: this could explain part of the deviation existing between $-R_{uT}$ and unity, namely for low Reynolds numbers.

(b) For various flows, including the boundary layer, Gaviglio *et al.* (ref. [12], p. S187) have verified that equation (20) or equation (21) apply even when $\partial\bar{p}/\partial x \neq 0$, in conformity with the analysis of the third case described in par. 2.2.1.

(c) None of the experiments confirmed the approximate equation (19), $\sqrt{(\overline{T_t'^2})} = 0$ (cf. Kistler [7]). Morkovin [5] regarded this as the missing key that would explain the SRA. Paradoxically, however, the hypothesis $T_t' = 0$ has been attributed to this author (cf. refs. [13, 17]). We recall that $\sqrt{(\overline{T_t'^2})}$ must be compared with $\sqrt{(\overline{T'^2})}$, or with $(\tilde{u}/c_p)\sqrt{(\overline{u'^2})}$ according to equation (15) and that the ratio $\sqrt{(\overline{T_t'^2})}/\sqrt{(\overline{T'^2})}$ is most often only slightly less than 1. How then can equation (20) be compatible with $\sqrt{(\overline{T_t'^2})} \neq 0$? In attempting to explain this, Debièvе [14] writes equation (18b) in the form of a double implication

$$T_t' = 0 \Leftrightarrow \begin{cases} (\sqrt{(\overline{T'^2})}/\tilde{T}) = (\gamma-1)M^2(\sqrt{(\overline{u'^2})}/\tilde{u}) & (24) \\ -R_{uT} = 1 & (25) \end{cases}$$

and demonstrates that, provided the SRA relation (24) is verified

$$R_{uT} = (\overline{T_t'^2}/\overline{T'^2}) - 1 \neq -1 \qquad (26)$$

then follows. In separate works (refs. [15, 16]) Gaviglio observes that, in a more general manner, when the rule of addition for two random variables is applied to equation (15) defining $T_t'$, the result is written

$$\sqrt{(\overline{T_t'^2})} = \left(\overline{T'^2} + \frac{\tilde{u}}{c_p}\overline{u'^2} + 2\frac{\tilde{u}}{c_p}\sqrt{(\overline{u'^2})}\sqrt{(\overline{T'^2})}R_{uT}\right)^{1/2}. \qquad (27)$$

This relation is confirmed (Figs. 3(a) and (b)) for a triangle MOP whose sides are equal to $\hat{T}_t' = \sqrt{(\overline{T_t'^2})}/\sqrt{(\overline{T'^2})}$, $\hat{T}' = 1$ and

$$\hat{u}' = (\gamma-1)M^2\frac{\sqrt{(\overline{u'^2})}/\tilde{u}}{\sqrt{(\overline{T'^2})}/T}$$

and whose opposite angles have a cosine of $-R_{uT}$, $-R_{T_t u}$ and $R_{T_t T}$, respectively. Condition (19) therefore appears sufficient but not necessary in order to satisfy equations (20)–(22). For example, the relation $\sqrt{(\overline{T_t'^2})} = 0$ would be confirmed for an ideal sound wave field, but not for a rotational, non-isentropic field (cf. Section 4).

Examination of Fig. 3(b) reveals that this construction applies to heated flows, even at low speeds, and that it illustrates the distinction, often poorly discerned, to be made between $\hat{T}_t'$ and $\hat{T}'$ which have similar standard deviations, but are different due to the influence of $\hat{u}'$. Since it is purely local, this construction also applies to the study of signals filtered in a common frequency band.

### 2.3. *The need for new models of the velocity–temperature relationship*

It has been shown (par. 2.1) how, within the boundary layer, the existence of high dissipation due to viscosity precludes the simple establishment of a theoretical and (too) strict analogy between enthalpy and velocity fluctuations, and how this problem led Young and Morkovin to formulate the SRA which, paradoxically, is expressed by relations that are just as strict between $u'$ and $T'$. To avoid this shortcoming,

† Since a heat flux exists in the absence of a heat source applied at the wall, the wall is not, strictly speaking, 'adiabatic'.

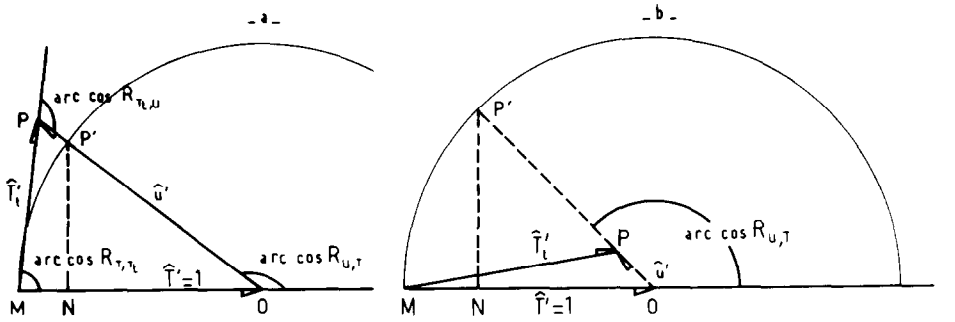


FIG. 3. Graphic representation of velocity and temperature fluctuations. (a) Supersonic boundary layer on a quasi-adiabatic wall. (b) Subsonic boundary layer on a heated wall.

an attempt has been made [13, 17] to demonstrate how these relationships can stem from known physical mechanisms of turbulent transfer and diffusion, at the same time avoiding reference to any models that are valid for perfect fluids, as these are incompatible with the rotational nature of the turbulent field.

Following the conclusions of Morkovin [5], the next part of this presentation assumes that these mechanisms, related to the properties of turbulence, are hardly influenced by compressibility which, although displayed in the mean motion, presents no substantial source of vorticity. Only in further reflections will the study examine the effects of compressibility in fluctuating motion which, moreover, will be explained once again by the mechanism recalled above.

Under no circumstances is the physical study of phenomena represented in the form of a model for flow calculation, as the purpose here is only to facilitate the introduction of these physical hypotheses into existing models.

## 3. SCHEMATIC MODEL BASED ON THE HYPOTHESIS OF AN ISOBARIC TURBULENT FIELD

### 3.1. *Large-scale movements in the boundary layer*

Werle's films [18] show that in free turbulent flows, and also in wall turbulent flows, large-scale movements occur in a plane normal to the mean flow, and in this case normal to the wall. These phenomena appear to be related to the 'bursting' phenomenon that seems to affect the boundary layer regardless of its Mach number. Filmed in the early 1950s by Weske and Theodorsen, cited by Head and Bandyopadihay [19], this phenomenon has since been visualized, photographed, and analyzed by several authors such as Kline *et al.* [20], Kim *et al.* [21], Antonia [22], Chen and Blackwelder [23], and Cantwell [24] for low-speed flows; and by Zakkay *et al.* [25], Owen and Horstman [26], Deckker and Weekes [27], and Deckker [28] for compressible flows. The bursting phenomenon has not been examined in the present study, but has simply been recalled to assist in providing a schematic view of boundary layer properties (cf. par. 3.2 and Section 4), hence only a few characteristics have been mentioned herein.

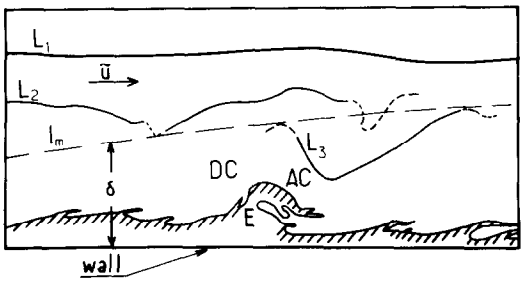


FIG. 4. Organized structures: E, burst; DC, AC, decelerated, accelerated flow; $l_m$, conventional mean boundary limit of the layer; $L_1$, particle emission path outside the turbulent region; $L_2$, $L_3$, particle emission path inside the turbulent region.

Large-scale movements are related to the presence of longitudinal eddies (streaks) produced randomly near the wall. Multitudes of concentrated eddies are ejected in loop, horseshoe, and hairpin shapes of various length, depending on the Reynolds number, and inclined on the wall to about 45°. These eddies burst in the inner region ($y/\delta \lesssim 0.15$) and sometimes in the outer region ($y/\delta \lesssim 0.4$), causing small-scale turbulence in the bursting process. This phenomenon is then followed by a fluid sweep with greater velocity and lower temperature than the bursts, and originating from the region near the outer boundary. These structures, illustrated in Fig. 4, alter the regularity of both the paths of emission and the isochronous lines used to visualize them [19]. Their motion, showing strong three-dimensionality, could be related to that of the superlayer. The production of turbulence, of friction within the boundary layer, etc. depends to a great extent on these movements.

An example drawn from visual examinations conducted at the I.M.S.T. by Daïen [29] is provided in Fig. 4. Taken at a low Reynolds number ($\mathscr{R}_\delta = 4900$), this representation shows an eddy in upward motion moving towards the outer region before it bursts.

As the properties recalled here seem to be relatively

independent of the Mach number, it appears possible to use them as a basis for a general schematic representation (see ref. [26]).

### 3.2. *Schematic model*

(a) The above considerations lead to a distinction, albeit arbitrary, between large- and small-scale components of velocity and temperature. Only large-scale movements will be taken into consideration in the present. Large-scale structures remain coherent over a length $L_y$ determined on the basis of space–time correlation measurements made at points $P(y)$ and $P'(y')$ on the same $Y$-axis normal to the wall. $L_y$ is written as

$$L_y = \int_{y'=0}^{\infty} \frac{\overline{u'(y,t)u'(y',t)}}{\sqrt{(\overline{u'^2}(y,t))}\sqrt{(\overline{u'^2}(y',t))}}\,\mathrm{d}y'.$$

They may be reasonably estimated from measurements published by Favre *et al.* [30]. Near the wall $L_y/\delta$ appears to have a value of approximately 0.2 and increases as $Y$ increases, reaching 0.4 at the free boundary.

Large-scale movements may be described by the 'flutter' diagram proposed by Burnage (cf. Burnage and Gaviglio [31]) for a supersonic laminar flow oscillating transversely in a random manner. The mean velocity and temperature profiles oscillate as a single block ahead of the probe set up at P (cf. Fig. 1). This probe acquires signals $u'_r$ and $T'_r$ 'induced' in the instantaneous relative displacement

$$u'_r = \frac{\partial \tilde{u}}{\partial y} y', \qquad T'_r = \frac{\partial \tilde{T}}{\partial y} y'. \tag{28a}$$

Phase opposition occurs between $u'_r$ and $T'_r$ since the mean gradients are of opposite signs: the correlation coefficient $-R_{uT}$ is therefore equal to 1. The standard deviation for fluctuation $y'$ is written as

$$\sqrt{(\overline{y'^2})} = \frac{\sqrt{(\overline{u'^2_r})}}{\partial \tilde{u}/\partial y} = \frac{\sqrt{(\overline{T'^2_r})}}{\partial \tilde{T}/\partial y}. \tag{28b}$$

The formulation proposed here requires at least that $\sqrt{(\overline{y'^2})}$ be less than coherent length $L_y$ in order to be confirmed. Scales that are characteristic of the *overall* signal are defined as

$$l_u = \frac{\sqrt{(\overline{u'^2})}}{\partial \tilde{u}/\partial y} \tag{29}$$

$$l_T = \frac{\sqrt{(\overline{T'^2})}}{\partial \tilde{T}/\partial y}. \tag{30}$$

This assumes that the ratio $l_T/l_u$ is equal to 1, which is in fact the case if small-scale fluctuations, not taken into account by signals $u'_r$ and $T'_r$, alter these signals in approximately equal proportions. As concerns the correlation coefficient $-R_{uT}$, in the case of low-speed flows, these fluctuations reduce its value. In Section 4 it will be shown that compressible flows provide quite different results. The premises of the present formulation, expressed by equations (29) and (30), are therefore akin to those of Prandtl's mixing length representation applied to both velocity and thermal fields.

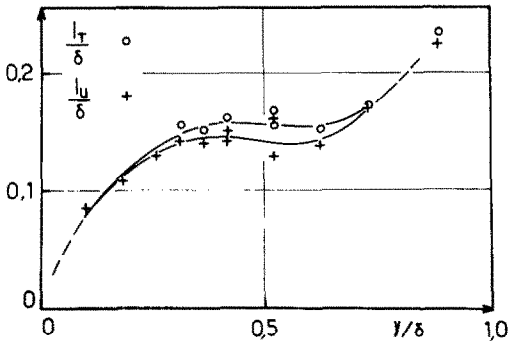


FIG. 5. Characteristic lengths of temperature and velocity fluctuations across the boundary layer. Quasi-adiabatic wall, $M_e = 2.32$.

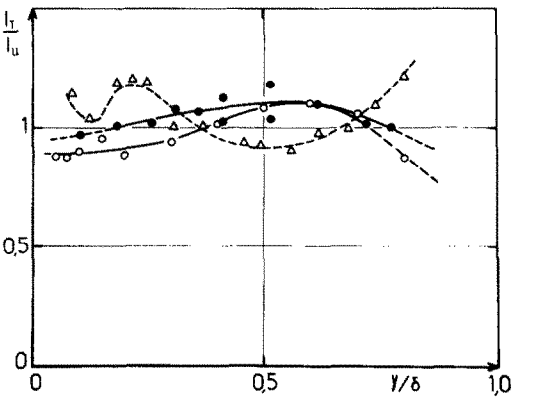


FIG. 6. Ratio of characteristic lengths of temperature and velocity fluctuations across the boundary layer: ○, ref. [32]; △, ref. [33]; ●, ref. [34].

(b) Predictions of this representation are reasonably confirmed by experimental results. Figure 5 concerns a supersonic boundary layer on a quasi-adiabatic wall. The conditions are the same as for Fig. 7. Figure 5 shows that for any value of $y/\delta$, $l_u/\delta$ and $l_T/\delta$ have neighbouring values more than two times lower than $L_y/\delta$. Figure 6 pertains to three very different flows: a supersonic flow on a quasi-adiabatic wall (Debiève [32], as above); a hypersonic flow on a cooled wall (Laderman and Demetriades [33], same conditions as Fig. 8); and a supersonic flow on a slightly heated wall (Fulachier [34]). In each case, the ratio $l_T/l_u$ is practically constant within $\pm 10$ to 15%, for any value of $y/\delta$, excluding the viscous sublayer. Deviations are no greater than measurement errors, which does not imply, however, that they may be explained by the latter.

It should also be pointed out that the basis of the new schematic model conforms to the rules recalled

by Launder and Spalding (ref. [35], readings 2 and 3) that must be observed if the mixing length hypothesis is to express correctly the turbulent transfer of scalar or vector quantities.

(c) The schematic representation consists of writing equations relating $T'$ to $u'$, based on equations (29) and (30)

$$\frac{\sqrt{(\overline{T'^2})}}{\sqrt{(\overline{u'^2})}} \simeq -\frac{\partial\tilde{T}/\partial y}{\partial\tilde{u}/\partial y} = -\frac{\partial\tilde{T}}{\partial\tilde{u}} \tag{31}$$

or

$$\frac{\sqrt{(\overline{T'^2})}/\tilde{T}}{\sqrt{(\overline{u'^2})}/\tilde{u}} \simeq -\frac{\mathrm{d}\log\tilde{T}}{\mathrm{d}\log\tilde{u}} \tag{32}$$

or

$$\frac{\sqrt{(\overline{T'^2})}/\tilde{T}}{(\gamma-1)M^2\sqrt{(\overline{u'^2})}/\tilde{u}} \simeq \left(1-\frac{\partial\tilde{T}_t}{\partial\tilde{T}}\right)^{-1} \tag{33}$$

equation (33) being deduced from equations (32) and (14).

If it is assumed that $\tilde{T}_t(y/\delta)$ is strictly invariant, equation (33) would coincide with equation (21), which would not be the case even if the wall were adiabatic. Neither would this apply in the case of a non-heated wall which, by means of conductivity in the wall supports, maintains a temperature $T_w$ slightly greater than the 'friction' temperature $T_f \leqslant T_{te}$ (cf. nomenclature). Therefore, the term $(1-\partial\tilde{T}_t/\partial\tilde{T})^{-1}$ is not equal to 1, but does approach this value. In general it may take on large values. It should be noted that the length of segment OP $= \tilde{u}'$ in Fig. 5 is equal to $(1-\partial\tilde{T}_t/\partial\tilde{T})$.

*Remark.* The present analogy does not assign a value to the correlation coefficient $(-R_{uT})$, but it does express that it cannot be equal to 1.

3.3. *Confrontation between analogies and experiment*

3.3.1. *Supersonic flow.*

(a) Case of the quasi-adiabatic wall.

Figure 7 illustrates the case of a boundary layer developing on a nozzle wall (cf. ref. [32]). Conditions are as follows:

$(\partial\bar{p}/\partial x) = 0$, $M_e = 2.32$

$T_{te} = 293\,\mathrm{K}$, $T_w = 284.6\,\mathrm{K}$, $T_f = 278\,\mathrm{K}$

$\delta_{995} = 9.6\,\mathrm{mm}$, $\theta = 0.73\,\mathrm{mm}$, $\mathscr{R}_e = 5650\,\mathrm{mm}^{-1}$.

The free conventional boundary is the same for the velocity and temperature fields. Satisfactory agreement is found between the present analogy and experiment, especially for the inner region. Results coincide fairly well with equation (21) and even more so with equation (23), the so-called 'extended SRA solution' (cf. par. 2.2.1) which takes into account a residual heat flux.

(b) Case of the heated wall.

In the absence of boundary layer behaviour on a wall heated to high temperatures, the present analogy,

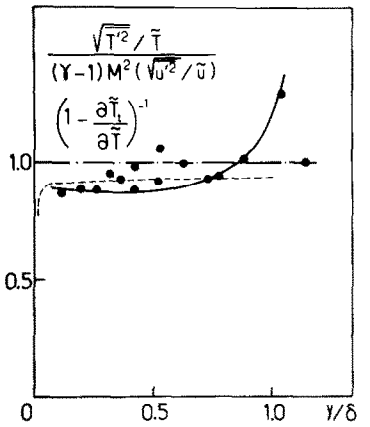


FIG. 7. Comparison of results (adiabatic wall, $M_e = 2.3$): ●, experiment; ——, present analogy; – – –, 'extended SRA solution'.

equation (33), has been applied to average profiles of velocity and temperature, not far from internal equilibrium, but calculated† using a mixing length method. The conditions are the same as those for the preceding figure, but three wall temperatures have been considered

$$T_w = 280\,\mathrm{K} \quad (T_w/T_f) = 1$$

(the results practically coincide with those of Fig. 7)

$$T_w = 420\,\mathrm{K} \qquad (T_w/T_f) = 1.5$$

$$T_w = 560\,\mathrm{K} \qquad (T_w/T_f) = 2.$$

Results are shown on Fig. 9, along with those of Fig. 8 discussed below. The extended SRA solution applied to cases of heated flow does not provide satisfactory results here, due to the high temperatures imposed at the wall; it therefore has not been presented in the figure. Discussion of Fig. 9 is presented in par. 3.3.3.

3.3.2. *Hypersonic flow on cooled wall.* For the case shown in Fig. 8, flow characteristics (cf. ref. [33]) are the following:

$(\partial\bar{p}/\partial x) = 0$, $M_e = 9.37$

$T_{te} = 792\,\mathrm{K}$, $T_w = 304\,\mathrm{K}$, $T_f = 758\,\mathrm{K}$

$\delta_{995} = 6.1\,\mathrm{in.}$ (15.49 cm), $\theta = 0.29\,\mathrm{in.}$ (0.72 cm), $\mathscr{R}_e = 12{,}700\,\mathrm{mm}^{-1}$.

This figure also illustrates the comparison between the values of the first member of equation (33), drawn from the experiment, and those of the second member which represent the proposed analogy, as a function of thickness $\bar{\delta} = 4.05\,\mathrm{in.}$ (10 cm) defined by the authors on the basis of the standard deviations of the turbulent fluctuations ('r.m.s. thickness'). Two sets of measurements are presented, obtained using two different hot-

† By the O.N.E.R.A. centre C.E.R. in Toulouse; results kindly provided by Mr Leuchter of the Aerodynamics Division.

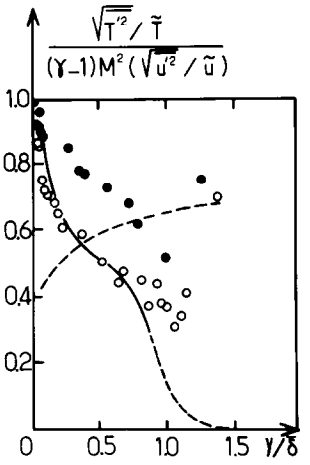


FIG. 8. Comparison of results (cooled wall, $M_e = 9.4$): ○, ●, experiment (two different wires); ——, present analogy; – – –, extended SRA solution.

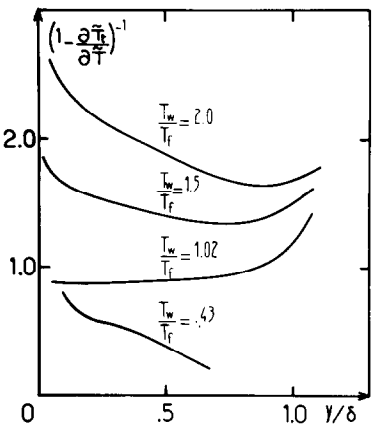


FIG. 9. Distributions through the boundary layer of the ratio of temperature and velocity fluctuation levels. Influence of the wall temperature.

wire probes. The differences between the two sets are noticeable, but normal, given the difficulties encountered in studying hypersonic flows. These problems involve both experimental conditions, namely calibration of the probes, and methodology, especially in interpreting measurement results, which is complicated by the existence of a high level of pressure fluctuations at the wall (cf. original works by Kovasznay [6] and Morkovin [36]; the analysis made by Bradshaw [37]; and the paper by Laderman and Demetriades). For both sets of measurements, the ratio

$$\frac{\sqrt{(\overline{T'^2})}/\tilde{T}}{(\gamma-1)M^2(\sqrt{(\overline{u'^2})}/\tilde{u})}$$

approaches 1 when $(y/\delta) \to 0$, and decreases as the distance from the wall increases. The present analysis is in rather good agreement with one set of measurements, namely as concerns $(y/\delta) < 3/4$. The extended SRA solution, however, applies poorly in the case of the cooled wall, because it is not adapted to the case of a strong temperature heat flux at the wall.

3.3.3. *Summary of results provided by application of the present representation to supersonic flows.* Figure 9 summarizes the above results, indicating in a qualitative manner how the ratio

$$\frac{\sqrt{(\overline{T'^2})}/\tilde{T}}{(\gamma-1)M^2(\sqrt{(\overline{u'^2})}/\tilde{u})}$$

represented by $(1-\partial\tilde{T}_t/\partial\tilde{T})^{-1} = \hat{u}'$ evolves through the boundary layer vs temperature gradients imposed at the wall. The difference to one were highly negative for $T_w/T_f = 0.43$; practically nil for $T_w/T_f = 1.02$; and highly positive for $T_w/T_f = 1.5$ and 2. Referring to Fig. 3, it may be observed that the more the wall is heated, the more point P approaches point O. Figure 3(b) could represent the case of a supersonic flow with a strong temperature heat flux.

3.3.4. *Application of the present analysis in low-speed flow on a slightly heated wall.* The experiments conducted by Fulachier [34] were carried out on a flat plate with a dynamic leading edge. A low heat source was imposed a short distance ahead of this edge, and conditions were as follows:

$(\partial\bar{p}/\partial x) = 0$, $M_e = 0.035$

$T_e = 293\,\text{K}$, $T_w = 315\,\text{K}$

$\delta = 62\,\text{mm}$, $\theta = 5.98\,\text{mm}$, $\mathscr{R}_e = 840\,\text{mm}^{-1}$.

At subsonic speeds the present analogy was applied in the form

$$\frac{\sqrt{(\overline{T'^2})}}{\sqrt{(\overline{u'^2})}}\frac{\partial\tilde{u}}{\partial\tilde{T}} = 1 \tag{34}$$

as well as in the 'attenuated form' of the so-called 'exact analogy'

$$\frac{\sqrt{(\overline{T'^2})}}{\sqrt{(\overline{u'^2})}}\frac{u_e}{T_w - T_e} = 1. \tag{35}$$

Comparisons with the experiment are given in Fig. 10. Equation (34) is confirmed correctly for the mean plot within $\pm 12\%$ for any value of $y/\delta$. The same is true for equation (35) where $y/\delta < 0.5$, but at greater distances the deviations are substantial. This seems to be explained by the slight difference existing between the origin of the dynamic field and that of the thermal field.

3.4. *Comments on applications of the present analogy*

3.4.1. The proposed schematic model cannot be applied to $T_t'$ in the same manner as it is applied to $T'$ and $u'$. If this were possible, one could define a distance $l_{T_t}$ such that $\sqrt{(\overline{T_t'^2})} = l_{T_t}(\partial\tilde{T}_t/\partial y)$; this cannot be done because of the non-linear form of equation (27). Moreover, there is no similarity between the total enthalpy and velocity profiles, as demonstrated by the results of Kistler [7], Debièvre [32] and others.

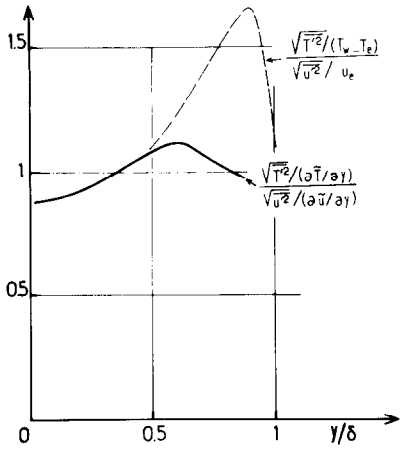


FIG. 10. Comparison of results: —·—·, theoretical value, 1; ——, present analogy, equation (31); – – –, conventional analogy, equation (11).

3.4.2. The present analogy can be used to characterize the evolution of the entropy mode between two known states of the boundary layer, 1 and 2, corresponding, respectively, to a quasi-adiabatic wall ($T_w/T_f \simeq 1$) and a heated or cooled wall ($T_w/T_f = 2$ in the example below). This can be achieved by finding the mean temperature distributions in each case, either through experimentation or calculation, and applying equation (33) to states 1 and 2. To simplify, it is admitted that the Reynolds number is fairly high. Under these conditions, an addition of heat, modifies $\delta$ and $M$ (e.g. from 10 to 15%) but does not change velocity turbulent intensity significantly. This leads to

$$\frac{(\sqrt{(\overline{T'^2})}/\tilde{T})_2}{(\sqrt{(\overline{T'^2})}/\tilde{T})_1} \simeq \frac{M_2^2\,[1-(\partial\tilde{T}_t/\partial\tilde{T})]_1}{M_1^2\,[1-(\partial\tilde{T}_t/\partial\tilde{T})]_2}.$$

Based on the experiments described in ref. [32] and the calculation of the same mean flow heated to high temperatures ($T_w/T_f = 2$, cf. par. 3.3.1.b and Fig. 9), results corresponding to a distance from the wall $y/\delta = 0.1$, $\sqrt{(\overline{u'^2})}/\tilde{u} = 0.1$ and $(\sqrt{(\overline{T'^2})}/\tilde{T})_1 = 0.055$, are as follows:

$$\frac{T_2}{T_1} \simeq 1.4, \qquad \left(\frac{\sqrt{(\overline{T'^2})}}{\tilde{T}}\right)_2 \Big/ \left(\frac{\sqrt{(\overline{T'^2})}}{T}\right)_1 \simeq 2,$$

$$\frac{(\sqrt{(\overline{T'^2})})_2}{(\sqrt{(\overline{T'^2})})_1} \simeq 3.$$

It appears clearly that heating the wall strongly increases the heat turbulence level.

3.4.3. The gradient-based representation associated with the geometric diagram presented in Fig. 3 is of interest as it may also contribute to simplify certain measurements. Experimentation may be formulated on the basis of quantities measured using complementary means and methods such as pressure probes, hot-wire anemometry and laser Doppler velocimetry. As an example, $\tilde{T}_t$ and $\sqrt{(\overline{T_t'^2})}$ may be obtained using a constant-temperature hot-wire anemometer; $\tilde{u}$ and $\sqrt{(\overline{u'^2})}$ may be obtained through laser Doppler velocimetry (cf. Eléna *et al.* [38]). The three sides of the triangle are therefore defined as

$$\mathrm{MO} = \hat{T}' = 1$$

$$\mathrm{OP} = \hat{u}' = \left(1 - \frac{\partial\tilde{T}_t}{\partial\tilde{T}}\right)^{-1}$$

where $\tilde{T}$ is deduced from equation (14)

$$\mathrm{MP} = \hat{T}_t' = \frac{\sqrt{(\overline{T_t'^2})}}{\sqrt{(\overline{T'^2})}}$$

where $\sqrt{(\overline{T'^2})}$ is taken from equation (33).

Results must be interpreted with caution, as measurement accuracy is different for each type of apparatus and method used.

3.4.4. Lastly, it is recalled that the application of the proposed schematic model (cf. ref. [13], par. 3.5) provides the following relationship between the turbulent Prandtl number and coefficients of correlation:

$$Pr_t \simeq -\frac{R_{uv}}{R_{Tv}}.$$

This is satisfactorily confirmed through experimentation in the case of low-speed equilibrium boundary layers.

## 4. EFFECTS OF COMPRESSIBILITY

4.1. *Review*

(a) The preceding study confirms Morkovin's idea [5] that in an equilibrium boundary layer, the mechanisms of turbulence production, diffusion and dissipation do not depend primarily on compressibility, although this phenomenon does have an influence on the mean temperature distribution. One interpretation [26] of results from measurements conducted at a fairly high Mach number ($M_e = 7.2$) confirmed that the structure of the boundary layer is such that "... turbulent production ... is consistent with previous results obtained in incompressible flow". This idea has made it possible to establish a model of the velocity–temperature relationship (par. 3.2) in the presence or absence of heat at the wall. It is nonetheless important to point out that results could be very different for flows strongly out of equilibrium, as for interactions between turbulence and shock or relaxation waves (cf. refs. [11, 12, 16, 32, 39]). The present is an attempt to specify how compressibility acts on the relationship between fluctuations of velocity, temperature, and pressure. This requires a brief review of certain principles.

(b) In addition to isobaric fluctuations of velocity $q_w'$ and temperature $T_{is}'$, respectively characterized as rotational and isentropic and transported by the flow [8], there exist [6] pressure fluctuations $p'$ which are propagated by waves that cross the streamlines. In

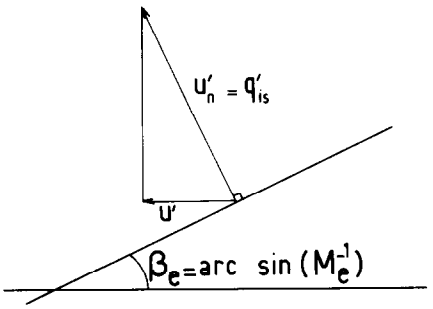


FIG. 11. Mach wave: isentropic wave front, and irrotational velocity fluctuations.

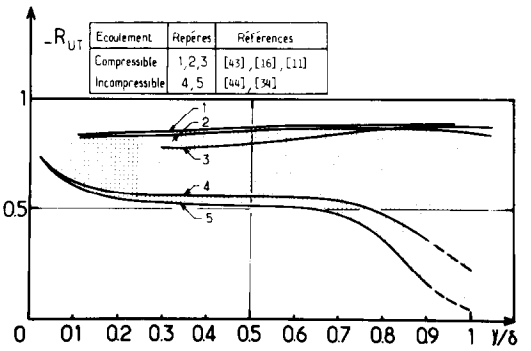


FIG. 12. Distributions, through the boundary layer, of correlation coefficient $-R_{uT}$ for compressible and incompressible flows.

a wave model, the fluctuation $p'$ is associated with irrotational velocity fluctuations $q'_{ir}$, and isentropic temperature fluctuations $T'_{is}$; the latter can exist even in situations where a wave model does not hold. One can write the following (Finzi and Pastori [40]):

$$\mathbf{q}' = \mathbf{q}'_w + \mathbf{q}'_{ir} \tag{36}$$

(omitting 'induced' velocity for simplification); and

$$T' = T'_s + T'_{is}. \tag{37}$$

Applying the law of plane waves gives

$$p' = \bar{\rho} a q'_{ir} \tag{38}$$

and the law of isentropy

$$\frac{T'_{is}}{\bar{T}} = \frac{\gamma - 1}{\gamma} \frac{p'}{\bar{p}}. \tag{39}$$

Density fluctuations are separated into two terms such that $\rho' = \rho'_s + \rho'_{is}$, where $\rho'_s$ obeys law (4) and $\rho'_{is}$ law (39) (cf. Gaviglio [41]). Within the boundary layer, the level of pressure fluctuations increases rapidly as the external Mach number rises. Outside the superlayer, fluctuations $\mathbf{q}'_{ir}$, $T'_{is}$ and $\rho'_{is}$ predominate, corresponding to radiated sound waves. Based on a theory put forward by Phillips (1960), Laufer [42] showed that these waves seem to be generated by 'sources' transported at a velocity $u_s$, close to $\tilde{u}(y/\delta)$, that are supersonic with respect to the outer flow: $u_e - u_s \geqslant a_e$. At a large distance from the wall, these sources are inclined at an angle

$$\beta = \arcsin \frac{1}{M_e\left(1 - \dfrac{u_s}{u_e}\right)}.$$

If $u_s = \tilde{u}$ (assumed in this case for the sake of simplicity) these would be 'Mach waves'. According to equations (38) and (39), $p'$, $T'_{is}$ and $\mathbf{q}'_{ir}$ provide a correlation of 1. Figure 11 shows schematically that a hot-wire probe perpendicular to the figure plane is influenced, not by velocity $\mathbf{q}'_{ir}$ normal to the wave plane, but by its component $u'_{ir}$ of $\mathbf{q}'_{ir}$. This results in

$$R_{pq} = R_{pT} = 1 \quad \text{but } R_{pu} = -1.$$

### 4.2. *Experimental presumptive evidence of compressibility effects*

Compressibility effects may be recognized by comparing results obtained in supersonic flow with others provided at low speed. The moderate differences observed in the standard deviations of $u'$ and $T'$, when appropriately represented in a dimensionless form [7], are not commonly attributed to these effects: this hypothesis is admitted in the present paper in order to establish an approximation. More significant differences are displayed by distributions of the correlation coefficient $-R_{uT}$, which is to date the only correlation to be measured with any reasonable amount of accuracy. These differences cannot be explained by measurement errors.

4.2.1. *Evolution of the velocity–temperature correlation coefficient across the boundary layer.* Figure 12 represents the evolution of $-R_{uT}$ across the boundary layer in various experiments. At supersonic speeds (curves 1 [43] and 2 [16], $M_e = 2.3$; curve 3 [11], $M_e = 1.77$) this coefficient is close to $-0.8$ and increases as $y/\delta$ rises. At large distances, the measurements of radiated 'noise' [42] indicate that it approaches 1. At low speeds, however (curves 4 [44] and 5 [34]), $-R_{uT}$ decreases steadily as $y/\delta$ increases.

4.2.2. *Evolution of the velocity–temperature correlation coefficient as a function of wave number.* Figure 13 represents the evolution of $(-R_{uT})_n$ related to signals filtered in a narrow frequency band, as a function of wave number $k_1\theta$ per momentum thickness, for various Mach numbers $M_e$. At low speeds, $(-R_{uT})_n$ declines regularly as $k_1\theta$ increases, which corresponds to a 'loss of memory during the cascade process' from the largest structures to the smallest (cf. Bestion [39]). At supersonic speeds it declines less rapidly, and increases for the highest external Mach number. This type of evolution cannot be attributed to the fact that the distances from the wall $y/\delta$, and therefore the Mach number and the turbulence level, are not exactly the same, since the experiment shows that the results depend only slightly on these parame-

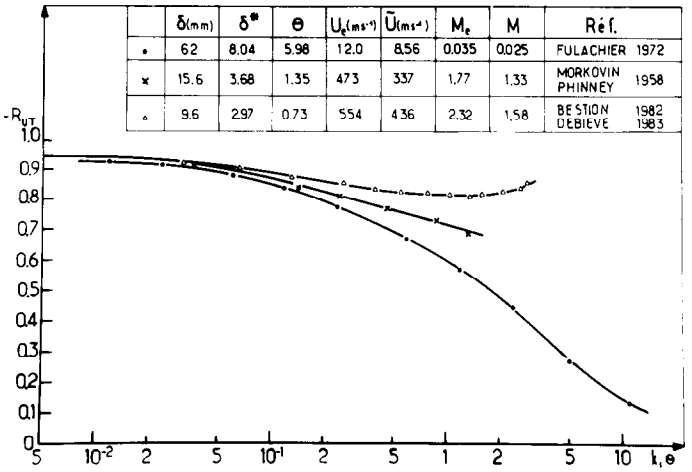


FIG. 13. Distributions of correlation coefficient $-R_{uT}$ vs wave number $k_1\theta$. Influence of the external Mach number.

ters (cf. ref. [32], Fig. 34; ref. [39], Figs. 70 and 72). This is also true for the ratio

$$\left[\frac{\sqrt{(\overline{T'^2})}/\tilde{T}}{(\gamma-1)M^2\sqrt{(\overline{u'^2})}/\tilde{u}}\right]_m$$

that expresses the relative levels of the fluctuations $u'$ and $T'$. Consequently, it may be assumed that the evolution is an effect of the external Mach number.

4.3. *Physical interpretation of experimental results*

In view of the above results, it appears necessary to assess the possible causes that could explain how compressibility is responsible for maintaining the high values of the velocity–temperature correlation coefficient. Two reasons seem to be related to properties of the coherent large-scale structures, and another to the internal intermittency of turbulence.

4.3.1. *Role of large-scale, quasi-organized structures.* Even before the existence of large-scale structures within compressible boundary layers was recognized (cf. par. 3.1), their presence was suspected and postulated in attempting to explain the sound radiation of these layers. From a Schlieren picture taken by James (1958), Laufer [45] inferred that these waves were due to short-lifetime 'sources'. Ffowcs Williams and Maidenik (ref. [46], p. 643) consider them as ...a form of balistic shock waves "attached to coherent regions of turbulence, or eddies, convected supersonically..." with respect to the outer flow. Since then, this presence within high-speed layers has been demonstrated by measurements [25, 26]; by visual observations in a shock tube [27, 28]; and by analysis of these documents [19]. For Deckker (private communication) these are regions with a high-density gradient since they appear clearly in Schlieren pictures. They are therefore inhomogeneous entities of strong vorticity, where mean velocity is less than in the ambient environment, and temperature higher. It is likely that, as at low speeds, they deform isochronous and emission paths [20, 29], which at supersonic speed would bring about the formation of zones of compression with shock on the back of the structures, and low gradient zones of relaxation on the front (Fig. 14). If this hypothesis† is correct, mean total temperature is practically constant: a hot-wire probe located alternately in an accelerated zone AC, and then in a decelerated zone DC (Fig. 4) records deviations of mean temperature and velocity of opposite sign such that, as per equation (14): $\Delta\tilde{T} = -(\tilde{u}/c_p)\Delta\tilde{u}$, resulting in a correlation of $-1$. Application of the 'flutter' diagram, equations (28)–(30), leads to the same result. The deviations mentioned above occupy a very wide frequency band, due to the fact that a wide dispersion exists in the production time of bursts and in the intervals separating them [20], and also due to the abrupt nature of the compression zones.

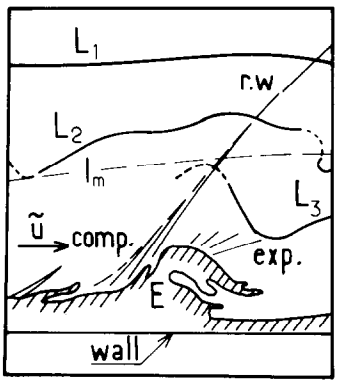


FIG. 14. Compression (comp.) and expansion (exp.) waves around a large structure, resulting in radiated Mach waves (r.w.), $l_m$, $L_1$ to $L_3$, as for Fig. 4.

† As is stated in ref. [46]: "...due to the convective motion of the coherent regions of turbulence...it is only to be expected that eddies moving supersonically should create rudimentary shock waves".

These deviations are superimposed on turbulent fluctuations $u'_\omega$ and $T'_s$ and on fluctuations $u'_{ir}$ and $T'_{is}$ whose properties were described in par. 4.1.b. Outside of the boundary layer, the radiated waves are emitted by 'sources' that are sufficiently close to the wall for their speed to be supersonic with respect to the outer flow.

This schematic model accounts for the fact that at supersonic speed, the correlation coefficient $-R_{uT}$ is sustained at high values throughout the boundary layer (Fig. 12) and approaches 1 at relatively large distances from the wall $y/\delta$ where measurements involve only acoustic waves. This implies that, due to compressibility, $\Delta\tilde{u}$ and $\Delta\tilde{T}$ replace the signals for which a loss of memory occurred in the cascade process. Actually, a physical model of this type can only provide a quite simplified picture of reality. Moreover, it would be false to believe that it is the only representation possible. Great caution is required in this domain: Ffowcs Williams [47] demonstrated that it is permissible to admit several solutions to the problem of localizing the noise sources and explaining their intensity. It is perhaps possible to avoid a questionable picture by accepting the assertion of Rayleigh [48] who states that "a region of altered compressibility acts like a simple source, a region of altered density like a double source".

4.3.2. *Effect of fluctuations at scales of dissipation.* Heat production within the high-speed turbulent boundary layer may be represented schematically as 'spots of entropy', borne from the intermittency of the locally high rate of fluid deformation inherent to small-scale turbulence. This deformation rate is in turn related to the pressure field. On these aspects of dissipation, one may consult Anselmet [49]. At any point in the flow, the enthalpy field therefore results from both the spread in volume caused by turbulence, and enthalpy produced locally. This mechanism does not appear to introduce any major signs of specificity levels of $u'$ and $T'$, as was noted in par. 4.2.2; it cannot be excluded that this could be due to the fact that the instrumentation frequency pass-band was limited to 340 kHz. It should therefore be asked whether the production of entropy spottiness could influence correlation coefficient $-R_{uT}$, obtained with or without filtering signals $u'$ and $T'$. According to Chu and Kovasznay [50], any addition of local heat—brought on in this case by dissipation and turbulent convection—increases the temperature and entropy of the fluid, causing it to expand. This expansion induces pressure waves in the surrounding environment (like those waves that cause the volume of a membrane to fluctuate). It is tempting to interpret this as one of the possible sources of the noise radiation by the boundary layer (previously mentioned with respect to Figs. 12 and 13) as well as one of the sources of fluctuation.

To summarize, of the three mechanisms that seem capable of maintaining correlation coefficient $-R_{uT}$ at a value close to 1, two have been shown to be related to the properties of large-scale quasi-organized structures, and the third to the small-scale internal intermittency of turbulence.

## 5. CONCLUSIONS

This work has set out to study the relationship between velocity and temperature fields within an equilibrium turbulent boundary layer at supersonic speeds where a heat flux is present at the wall.

We have reviewed reasons explaining why the classical Reynolds analogy between heat flux and momentum transfers cannot be applied to the compressible boundary layer, and how Young and Morkovin were led to develop the basis of the so-called 'strong Reynolds analogy' specific to high-speed flows. The highlights, paradoxes, and limitations of the SRA were clarified. Conclusions pointed to the need for a new model of the velocity–temperature relationship. This led to a proposal for a method of study that would give way to new analogy relations.

Conform to the hypothesis of Morkovin, the method first postulated that transfer mechanisms depend only slightly on the external Mach number. This method primarily takes into account the role of large-scale fluctuations that have been illustrated in various studies involving coherent structures and the bursting phenomenon. A 'flutter' representation, due to Burnage, was applied to this type of motion. This made it possible to confirm the premises of the Prandtl theory applied to flows with heat transfers, and led to a formula relating the velocity and temperature turbulence levels, the local Mach number and the mean gradients of velocity, temperature and total temperature. This formulation would coincide with the SRA relations in the unrealistic case of flow on an adiabatic wall; it is distinct, however, in that it contains a term that takes into account a heat flux at the wall, and provides a significant correction to the interpretation of experimental results concerning a non-heated, quasi-adiabatic wall. The new schematic model appears to apply reasonably well to the case of a cooled wall, which is not well represented by the SRA relations. It would be especially useful to test this model against results from detailed experiments conducted on a wall heated to high temperatures, but this data is as yet unavailable for supersonic flows. Examples of application have been given to illustrate the possibilities of this method in the field of measurement, and to demonstrate how it may be used to specify the evolution of temperature turbulence under the influence of an imposed heat flux at the wall.

An attempt was then made to discern the effects of compressibility on the velocity and temperature turbulent field. While the energy effect of pressure fluctuations is small, it appears clearly on distributions of the velocity–temperature correlation coefficient for the longitudinal component of velocity fluctuation.

This correlation remains high, sometimes close to $-0.8$, for the major portion of the thickness of the layer. The same correlation coefficient for signals filtered in narrow frequency bands stays in the same manner at high values, over a very wide wave number range per momentum thickness. It has been shown that these characteristics are specific to high speeds, and that they may be attributed in large part to the same causes that provoke boundary layer sound wave radiation. One of these causes is the presence of eddies in the flow that are referred to as 'bursts'. It seems likely that in supersonic flow, compression and relaxation waves develop in the area surrounding these bursts. Another possible cause could be the intermittency of small-scale velocity turbulence, responsible for creating entropy spottiness inside the flow. Both causes, perhaps interrelated, participate in the radiation of sound waves called Mach waves. It has been emphasized that this schematic representation is not to be understood in an absolute sense. It is to serve only as a reference in attempting to study, experimentally, the problem of the effects of compressibility on the relationship between velocity and temperature.

The preceding analysis should facilitate the study of various subjects related to heat and momentum transfer in high-speed turbulent boundary layers where a heat source is present at the wall. It has provided a certain number of elements that may contribute to finding answers to such questions as whether or not at supersonic speeds there exists, as at low speeds, a narrow spectral analogy between the thermal field and the dynamic field, a problem recently raised by Fulachier and Antonia [51]. This analysis may also be applied to the case of free-stream flows, and in a more general scope, to flows out of equilibrium.

*Acknowledgements*—The author is indebted to the scientists of I.M.S.T. for helpful discussions, and expresses his gratitude to Professors Antonia, Bradshaw, Ffowcs Williams and Young for their constructive criticism and advice. This paper was prepared in the framework of a contract between O.N.E.R.A. and I.M.S.T.

## REFERENCES

1. T. Cebeci and P. Bradshaw, *Physical and Computational Aspects of Convective Heat Transfer*. Springer, New York (1984).
2. A. Favre, L. S. G. Kovaszay, R. Dumas, J. Gaviglio et M. Coantic, *La turbulence en mécanique des fluides*. Gauthier-Villars, Paris (1976).
3. E. A. Brun, A. Martinot-Lagarde et J. Mathieu, *Mécanique des fluides*, Vol. 3. Dunod, Paris (1970).
4. A. D. Young, The equations of motion and energy and the velocity profile of a turbulent boundary layer in a compressible fluid, College of Aero., Cranfield, Rep. No. 42.
5. M. V. Morkovin, Effects of compressibility on turbulent flows, Coll. CNRS No. 108, Mécanique de la turbulence, pp. 367–380, CNRS ed., Paris (1962).
6. L. S. G. Kovasznay, Turbulence in supersonic flow, *J. Aeronaut. Sci.* **20**, 657–682 (1953).
7. A. L. Kistler, Fluctuation measurements in a supersonic turbulent boundary layer, *Physics Fluids* **2**(3), 290–296 (1959).
8. J. Laufer, Thoughts on compressible turbulent boundary layers, The Rand Corporation and Univ. of Southern California, Memo R.M. 5946-PR. (1969).
9. T. Cebeci and A. M. O. Smith, *Analysis of Turbulent Boundary Layers*. Academic Press, New York (1974).
10. P. Rebuffet, *Aérodynamique expérimentale*, Vol. 2. Dunod, Paris (1966).
11. J. P. Dussauge, Evolution de transferts turbulents dans une détente rapide, en écoulement supersonique, Doctorat es sciences physiques, I.M.S.T., Université d'Aix-Marseille II (1981).
12. J. Gaviglio, J. P. Dussauge, J. F. Debiève and A. Favre, Behaviour of a turbulent flow, strongly out of equilibrium at supersonic speeds, *Physics Fluids* **20**(10), S179–S192 (1977).
13. J. Gaviglio, Remarques sur l'analogie de Reynolds "deuxième manière" (Strong Reynolds Analogy). *Implications–Applications, Journées d'études "Ecoulements turbulents à masse volumique variable"* (Edited by L. Fulachier). Marseille (1985).
14. J. F. Debiève, Contribution à l'étude du comportement d'un écoulement compressible turbulent ($M = 2.3$) soumis à des gradients élevés de vitesse et de pression, Doctorat de spécialitée, Université d'Aix-Marseille II (1976).
15. J. F. Debiève, J. P. Dussauge et J. Gaviglio, Remarques sur une analogie entre les fluctuations turbulentes de vitesse et de température, en écoulements supersoniques, 4ème Congrès Français de Mécanique, Institut National Polytechnique de Lorraine, Université de Nancy I (1979).
16. J. F. Debiève, H. Gouin and H. Gaviglio, Momentum and temperature fluxes in a shock wave–turbulence interaction. In *Structure of Turb. and Heat and Mass Transfer* (Edited by Z. P. Zaric). Hemisphere, Washington D.C. (1981).
17. J. Gaviglio, Aspects physiques d'une analogie de Reynolds concernant les couches limites à vitesse supersonique, Coll. D.R.E.T.–O.N.E.R.A. Ecoulements turbulents compressibles, Poitiers (1986). Available from O.N.E.R.A., Paris.
18. H. Werle, Méthodes de visualisation des écoulements pour l'étude de l'aérodynamique à forte incidence, O.N.E.R.A. Film No. 1050, T.P. 1982–85, Paris (1982).
19. M. R. Head and P. Bandyopadihay, New aspects of turbulent boundary layer structure, *J. Fluid Mech.* **107**, 297–338 (1981).
20. S. J. Kline, W. C. Reynolds, F. A. Schraub and P. S. Runstadler, The structure of turbulent boundary layers, *J. Fluid Mech.* **30**(4), 741–773 (1967).
21. H. T. Kim, S. J. Kline and W. C. Reynolds, *J. Fluid Mech.* **50**(1), 133–160 (1971).
22. R. A. Antonia, Conditionally sampled measurements near the outer edge of a turbulent boundary layer, *J. Fluid Mech.* **56**(1), 1–18 (1972).
23. P. Chen and R. F. Blackwelder, Large-scale motion in a turbulent boundary layer: a study using temperature contamination, *J. Fluid Mech.* **89**(1), 1–31 (1978).
24. B. J. Cantwell, Organized motion in turbulent flow, *A. Rev. Fluid Mech.* **13**, 457–515 (1981).
25. V. Zakkay, V. Barra and C. R. Wang, The nature of boundary-layer turbulence at a high subsonic speed, *A.I.A.A. J.* **17**(4), 356–364 (1979).
26. F. K. Owen and C. C. Horstman, On the structure of hypersonic turbulent boundary layers, *J. Fluid Mech.* **53**(4), 611–636 (1972).
27. B. E. L. Deckker and M. E. Weekes, The unsteady boundary layer in a shock tube, *Proc. Instn mech. Engrs* **190**(11), 287 (1976).
28. B. E. L. Deckker, An investigation of some unsteady

boundary layers, by the Schlieren method, Int. Symp. on Flow Visualization, Ruhr-Universität, Bochum (1980).
29. E. Daïen, Contribution à l'étude d'écoulements turbulents par visualisations, Doctorat de spécialité, I.M.S.T., Université d'Aix-Marseille II, A and B (1980).
30. A. Favre, J. Gaviglio and R. Dumas, Space time double correlations and spectra in a turbulent boundary layer, *J. Fluid Mech.* **2**(4), 313–342 (1957).
31. H. Burnage and J. Gaviglio, Some measurements in the transitional supersonic wake of a transverse circular cylinder with emphasis on the effect of external noise, *Proc. Fluid Dynamics Panel Symposium*, Technical University of Lyngby, Denmark (1977).
32. J. F. Debiève, Etude d'une interaction turbulence-onde de choc, Doctorat es Sciences physiques, I.M.S.T., Université d'Aix-Marseille II (1983).
33. A. J. Laderman and A. Demetriades, Mean and fluctuating flow measurements in the hypersonic boundary layer over a cooled wall, *J. Fluid Mech.* **63**(1), 121–144 (1974).
34. L. Fulachier, Contribution à l'étude des analogies des champs dynamiques et thermiques dans une couche limite turbulente. Effet de l'aspiration, Doctorat es Sciences physiques, I.M.S.T., Univ. de Provence (Aix-Marseille) (1972).
35. B. E. Launder and D. B. Spalding, *Mathematical Models of Turbulence*, p. 169. Academic Press, New York (1972).
36. M. V. Morkovin, Fluctuations and hot-wire anemometry in compressible flows, Agardograph 24, North Atlantic Treaty Organization, Paris (1956).
37. P. Bradshaw, Compressible turbulent shear layers, *A. Rev. Fluid Mech.* **9**, 33–54 (1977).
38. M. Eléna, J. P. Lacharme and J. Gaviglio, Comparison of hot-wire and laser Doppler anemometry methods in supersonic turbulent boundary layers, Symposium on Laser Anemometry, 1985 Winter Annual Meeting, Miami Beach, Florida (1985).
39. D. Bestion, Méthodes anémométriques par fil chaud: application à l'étude d'interactions turbulence-gradient pression élevé, en couches limites à vitesse supersonique, Thèse de Docteur-Ingénieur, I.M.S.T., Université d'Aix-Marseille II (1982).
40. B. Finzi and M. Pastori, *Calcolo tensoriale* (Edited by N. Zanichelli). Bologna (1949).
41. J. Gaviglio, Sur quelques propriétés de la turbulence dans les écoulements supersoniques, *Rech. Aero.* No. 1971-1, 17–24 (1971).
42. J. Laufer, Sound radiation from a turbulent boundary layer, Coll. CNRS No. 108, Mécanique de la Turbulence, CNRS éd., pp. 381–393. Paris (1962).
43. M. Eléna, A. Borel and J. Gaviglio, Interaction couche limite-onde de choc. Couche limite initiale. Dispositif d'expériences. Rpt. ONERA (1977).
44. C. Rey, Effets du nombre de Prandtl, de la gravité et de la rugosité sur les spectres de turbulence cinématique et scalaire, Doctorat es sciences physiques. Ecole Centrale de Lyon, Labo. de Méca. des Fluides, Lyon (1977).
45. J. Laufer, Some statistical properties of the pressure field radiated by a turbulent boundary layer, *Physics Fluids* **7**(8), 1191–1197 (1964).
46. J. E. Ffowcs Williams and G. Maidenik, The Mach wave field radiated by supersonic turbulent shear flows, *J. Fluid Mech.* **21**(4), 641–657 (1965).
47. J. E. Ffowcs Williams, Aeroacoustics, *A. Rev. Fluid Mech.* **9**, 447–468 (1977).
48. J. W. S. Rayleigh, *Theory of Sound*, 2nd edn. Dover, New York (1894).
49. F. Anselmet, Intermittence interne de la turbulence pleinement développée: calcul de fonctions de structure d'ordres élevés et application à la combustion. Thèse de Docteur-Ingénieur, Univ. Sci. et Médicale, et Inst. Nat. Polytech., Grenoble (1983).
50. B. T. Chu and L. S. G. Kovasznay, Non linear interactions in a viscous heat-conducting compressible gas, *J. Fluid Mech.* **3**(5), 494–514 (1958).
51. L. Fulachier and R. A. Antonia, Spectral analogy between temperature and velocity fluctuations in several turbulent flows, *Int. J. Heat Mass Transfer* **27**, 987–997 (1984).

## LES ANALOGIES DE REYNOLDS ET L'ETUDE EXPERIMENTALE DU TRANSFERT DE CHALEUR DANS LA COUCHE LIMITE A VITESSE SUPERSONIQUE

**Résumé**—Pour le calcul des écoulements supersoniques, l'analogie de Reynolds classique doit être remplacée par une analogie plus spécifique. La "strong Reynolds analogy", due à Young et Morkovin, remplit assez bien ce rôle, mais seulement lorsque la paroi est quasi-adiabatique, c'est-à-dire non chauffée. Une forme plus générale de la SRA est ici proposée, qui tient compte de l'effet d'un flux de chaleur pariétal. Elle est basée sur des résultats concernant les mouvements à grande échelle dont la couche limite est le siège. Une schématisation convenable de ces mouvements conduit à une relation entre les niveaux de turbulence de température et de vitesse, et les caractéristiques moyennes de l'écoulement. Le rôle de la compressibilité sur le mouvement turbulent est en outre examiné.

## REYNOLDS ANALOGIEN UND DIE EXPERIMENTELLE UNTERSUCHUNG DER WÄRMEÜBERTRAGUNG IN DER UBER ÜBERSCHALLGRENZSCHICHT

**Zusammenfassung**—Überschallströmungen können nicht unter Benützung der klassischen Reynolds-Analogie berechnet werden; diese muß durch eine speziellere Form ersetzt werden. Die von Young und Morkovin vorgeschlagene Form der Reynolds-Analogie erfüllt diese Funktion annähernd, wenn die Wand quasi-adiabat ist, nicht aber wenn ein nennenswerter Wärmestrom vorhanden ist. Deshalb wird eine allgemeinere Darstellung vorgeschlagen. Auf der Grundlage von Ergebnissen, welche die in der Grenzschicht vorhandenen großräumigen Bewegungen berücksichtigen, stellt dieses schematische Modell eine Beziehung zwischen Temperatur, Turbulenzintensität der Geschwindigkeit und Charakteristik der Hauptströmung her. Gleichzeitig wird die Rolle der Kompressibilität bei der turbulenten Bewegung untersucht.

## АНАЛОГИИ РЕЙНОЛЬДСА И ЭКСПЕРИМЕНТАЛЬНОЕ ИЗУЧЕНИЕ ТЕПЛОПЕРЕНОСА В СВЕРХЗВУКОВОМ ПОГРАНИЧНОМ СЛОЕ

**Аннотация**—Сверхзвуковые течения нельзя рассчитать, применяя классическую аналогию Рейнольдса, которую необходимо заменить более точной. «Строгая аналогия Рейнольдса», предложенная Юнгом и Морковиным, выполняет эту роль приближенно только в случае квазиадиабатической стенки, но не пригодна при значительном тепловом потоке. Для преодоления этой трудности предложена более общая модель С учетом роли крупномасштабных движений в пограничном слое в этой схематической модели получена зависимость между тепловой и динамической интенсивностями турбулентности и средними характеристиками течения. Исследована также роль сжимаемости в турбулентном течении.